Available online at www.sciencedirect.com

ScienceDirect

Spectrochimica Acta Part A 66 (2007) 28–36

SPECTROCHIMICA ACTA PART A

www.elsevier.com/locate/saa

Synthesis, magnetic, spectral, and antimicrobial studies of Cu(II), Ni(II) Co(II), Fe(III), and UO_2(II) complexes of a new Schiff base hydrazone derived from 7-chloro-4-hydrazinoquinoline

Mostafa El-Behery*, Haifaa El-Twigry

Department of Chemistry, Education College for Girls, Scientific Departments, El-Montazah El-Gharby, Burydah, Qassim, KSA, Saudi Arabia

Received 12 November 2005; received in revised form 26 January 2006; accepted 13 February 2006

Abstract

A new hydrazone ligand, HL, was prepared by the reaction of 7-chloro-4-hydrazinoquinoline with *o*-hydroxybenzaldehyde. The ligand behaves as monoprotic bidentate. This was accounted for as the ligand contains a phenolic group and its hydrogen atom is reluctant to be replaced by a metal ion. The ligand reacted with Cu(II), Ni(II), Co(II), Fe(III), and UO_2(II) ions to yield mononuclear complexes. In the case of Fe(III) ion two complexes, mono- and binuclear complexes, were obtained in the absence and presence of LiOH, respectively. Also, mixed ligand complexes were obtained from the reaction of the metal cations Cu(II), Ni(II) and Fe(III) with the ligand (HL) and 8-hydroxyquinoline (8-OHqu) in the presence of LiOH, in the molar ratio 1:1:1:1. It is clear that 8-OHqu behaves as monoprotic bidentate ligand in such mixed ligand complexes. The ligand, HL, and its metal complexes were characterized by elemental analyses, IR, UV–vis, mass, and ^{1}H NMR spectra, as well as magnetic moment, conductance measurements, and thermal analyses. All complexes have octahedral configurations except Cu(II) complex which has an extra square-planar geometry, while Ni(II) mixed complex has also formed a tetrahedral configuration and UO_2(II) complex which formed a favorable pentagonal biprymidial geometry. Magnetic moment of the binuclear Fe(III) complex is quite low compared to calculated value for two iron ions complex and thus shows antiferromagnetic interactions between the two adjacent ferric ions. The HL and metal complexes were tested against one stain Gram positive bacteria (*Staphylococcus aureus*), Gram negative bacteria (*Escherichia coli*), and fungi (*Candida albicans*). The tested compounds exhibited higher antibacterial acivities.

© 2006 Elsevier B.V. All rights reserved.

Keywords: Schiff base ligand; Metal complexes; Antimicrobial; IR spectra; UV–vis spectra

1. Introduction

Schiff bases play an important role in inorganic chemistry as they easily form stable complexes with most transition metal ions. The development in the field of bioinorganic chemistry has increased the interest in Schiff base complexes, since it has been recognized that many of these complexes may serve as models for biologically important species [1–5]. The remarkable biological activity of acid hydrazides R–CO–NH–NH_2, a class of Schiff base, their corresponding aroylhydrazones, R–CO–NH–N=CH–R′, and the dependence of their mode of chelation with transition metal ions present in the living system have been of significant interest [6–12]. The coordination compounds of aroylhydrazones have been reported to act as enzyme inhibitors [13] and are useful due to their pharmacological applications [14–16]. Isonicotinic acid hydrazide (INH) is a drug of proven therapeutic importance and is used as bacterial ailments, e.g., tuberculosis [17]. Hydrazones derived from condensation of isonicotinic acid hydrazide with pyridine aldehydes have been found to show better antitubercular activity than INH [18,19]. Agarwal [18] investigated the coordinating ability of INH-derivatives with metal ions.

In the present investigation we describe the synthesis, characterization, and antimicrobial activitiy of transition metal complexes of Schiff base hydrazone containing the quinoline moiety, 7-chloro-4-(*o*-hydroxybenzilidenehydrazo)quinoline (HL).

2. Experimental

2.1. Reagents and malerials

$CuCl_2·2H_2O$, $NiCl_2·H_2O$, $FeCl_3·6H_2O$, $LiOH·H_2O$, salicylaldehyde and hydrazine hydrate (100%), and 8-hydroxyqui-

---

* Corresponding author. Tel.: +966 507112969.
E-mail address: behery_mostafa@hotmail.com (M. El-Behery).

1386-1425/$ – see front matter © 2006 Elsevier B.V. All rights reserved.
doi:10.1016/j.saa.2006.02.017

noline were either BDH or Merck chemicals and were used without further purification.

2.2. Synthesis of the organic ligand

2.2.1. 4,7-Dichloroquinoline

It was provided as commercial sample from El-Nasr-Company for pharmaceutical chemicals, Cairo, Egypt, and has been purified in laboratory as follows. Under warming and constant stirring, 10 g (10 mmol) of the sample was dissolved in 150 ml absolute ethanol. The solution was filtered while hot, and then allowed to cool. After that white cottony crystals were formed which were filtered and washed with 5–10 ml ethanol and then recrystallized from ethanol (70% yield, mp 82 °C). The crystals were stored in brown container to avoid light, which may affect it.

2.2.2. 7-Chloro-4-hydrazinoquinoline

To 10 g (5 mmol) of 4,7-dichloroquinoline dissolved in 20 ml ethanol, 25 ml (50 mmol) hydrazine hydrate (100%) in 30 ml absolute ethanol was added. The mixture was refluxed for 2 h. After 1/2 h, a golden yellow precipitate started to precipitate. After the refluxing time was reached, the mixture was allowed to cool for 6 h. The golden yellow precipitate was filtered and washed with 5 ml absolute ethanol and recrystallized from absolute ethanol (80% yield, mp 223–224 °C).

2.2.3. 7-Chloro-4-(o-hydroxybenzilidenehydrazo)quinoline

The ligand (HL) was synthesized as follows. 7-Chloro-4-hydrazinoquinoline, 2 g (1 mmol) was dissolved in 10 ml absolute ethanol. To this solution salicylaldehyde, 13 ml (1.1 mmol), was added. The reaction mixture was refluxed for 2 h. After cooling, the formed yellow precipitate was collected, filtered, and finally washed with 5–10 ml absolute ethanol and purified by recrystallization from ethanol (80%, mp 235 °C).

2.3. Synthesis of the metal complexes

A solution of metal salt dissolved in ethanol was added gradually to a stirred ethanolic solution of the ligand, HL, in the molar ratio 1:1. The reaction mixture was further stirred for 2–4 h to ensure the complete precipitation of the formed complexes. The precipitated solid complexes were filtered, washed several times with 50% (v/v) ethanol–water to remove any excess of the unreacted starting materials. Finally, the complexes were washed with diethyl ether and dried in vacuum desiccators over anhydrous $CaCl_2$. The reaction of uranyl salt was carried out in methanol as it dissolved better in this solvent. The preparations described were repeated in the presence of LiOH, as deprotonating agent in the molar ratio 1:1:1 (M:HL:LiOH) and its addition is a must in order to obtain such preparation with good yield of Ni(II), and binuclear iron complexes.

2.4. Synthesis of mixed ligand complexes

A mixture of 0.126 g (3 mmol) LiOH, H_2O, 0.898 g (3 mmol) HL, and 0.44 g (3 mmol) of 8-OHqu in 60 ml methanol was added to the metal salt (3 mmol), $CuCl_2\cdot 2H_2O$, $NiCl_2\cdot 6H_2O$, or $FeCl_3\cdot 6H_2O$ dissolved in the least amount of bidistilled water. The reaction mixture was refluxed for 5 h with constant stirring to ensure the complete formation of the metal complexes. The precipitated solid complexes were filtered and washed several times with 50% (v/v) methanol–water to remove any excess of the unreacted starting materials. Finally, the complexes were washed with diethyl ether and dried in a vacuum desiccator over anhydrous $CaCl_2$. The complexes obtained by this method are $[CuL(8\text{-OHqu})]\cdot H_2O$, $[NiL(8\text{-OHqu})]\cdot 3H_2O$, and $[Fe(L)(8\text{-OHqu})(Cl)(H_2O)]\cdot 2H_2O$ which are soluble in DMF, DMSO, and ethanol and partially soluble in 1,4-dioxan.

2.5. Analytical and physical measurements

Electronic spectra were recorded for solution of the ligand, HL, in DMF, and for the metal complexes as Nujol Mull on a Jasco UV–vis spectrophotometer model V-550 UV–vis. The IR spectra were recorded using KBr discs on FT-IR 1650 Perkin-Elmer Spectrometer. ^1H NMR spectra were carried out in DMF-d_6 at room temperature using TMS as internal standard on a Brucker 250 MHz spectrophotometer. Magnetic susceptibilities of the complexes were measured by the Gouy method at room temperature using a model MK1 Johnson Matthey. Alpha Products, magnetic susceptibility balance. The effective magnetic moments were calculated using the relation ($\mu_{\text{eff}} = 2.828 (\chi_m T)^{1/2}$ B.M., where χ_m is the molar susceptibility corrected using Pascal's constants for diamagnetism of all atoms in the compounds. The TG–DTA measurements were carried out on a Shimadzu thermogravimetric analyzer in dry nitrogen atmosphere and a heating rate of 10 °C/min using the TA-50 WS1 program. Mass spectra were recorded at 70 eV and 300 °C on an MS 5988 Hewlett-Packard mass spectrometer. Conductivities were measured in DMF solutions of the complexes (10^{-3} M) using a model LBR, WTWD-812 Weilheim Conductivity meter fitted with a model LTA100 cell. Analyses of the metals followed decomposition of their complexes with concentrated nitric acid. The resultant solution was diluted with distilled water and filtered to remove the precipitated ligand. The solution was then neutralized with aqueous ammonia solution and the metal ions titrated with EDTA. Analysis of the uranyl complex was carried out at the Central Laboratory for Environmental Quality Monitoring, CLQM, Kalubia, Cairo, Egypt. The complex was first dried and grinded followed by digestion by nitric–HF digestion mixture using Milestone Microwave Digester Model MLS 1200 Mega. The digestible uranium metal was analyzed using Perkin-Elmer ICP OES, Model Optima-3000 coupled with an Ultra Sonic Nebulizer, USN. Microanalyses of carbon, hydrogen, nitrogen, and chlorine were carried out at the Micro Analytical Center, Cairo University, Giza, Egypt.

2.6. Pharmacology

The in vitro evaluation of antimicrobial activity was carried out at Saudi Pharmaceutical Industries and Medical Appliance Corporation. The purpose of the screening program is to provide antimicrobial activity and bacteriostatic and fungistatic

Table 1
Elemental analyses, colour, yield, melting points, and molar conductance of HL and its corresponding metal complexes

Compound, M.F. (M.Wt.)	Elemental analysis, found (calculated) (%)					Colour	Yield (%)	mp (°C)	Molar conductance[a]
	C	H	N	Cl	M				
HL, $C_{16}H_{12}N_3OCl$ (297.5)	64.80 (64.53)	3.5 (4.03)	14.45 (14.11)	12.22 (11.93)	–	Yellow	94	225	–
$[Cu(L)_2]\cdot H_2O$, $C_{32}H_{24}N_6O_3Cl_2$ Cu (674.5)	56.82 (56.93)	3.75 (3.55)	12.60 (12.45)	10.50 (10.52)	10.20 (9.41)	Brown	60	>260 Decomposition	2.4
$[Cu(L)(8\text{-}OHqu)]\cdot H_2O$[b], $C_{25}H_{19}N_4O_3Cl$ Cu (522)	58.10 (57.47)	3.30 (3.64)	11.10 (10.73)	7.20 (6.80)	12.61 (12.16)	Light brown	80	>260 Decomposition	2.0
$[Ni(L)_2(OH_2)_2]\cdot 3H_2O$, $C_{32}H_{32}N_6O_7Cl_2$ Ni (742)	52.20 (51.75)	4.5) (4.31)	11.5 (11.32)	10.10 (9.57)	8.1 (7.95)	Orange-yellow	55	>250 Decomposition	2.6
$[Ni(L)(8\text{-}OHqu)]\cdot 3H_2O$[b], $C_{25}H_{23}N_4O_5Cl$ Ni (553.5)	54.80 (54.20)	4.60 (4.15)	11.00 (10.12)	7.00 (6.41)	11.00 (10.65)	Orange-yellow	76	>260 Decomposition	2.4
$[Fe(L)_2(OH_2)_2]\cdot NO_3\cdot 2H_2O$, $C_{32}H_{30}N_7O_9Cl_2$ Fe (783)	49.50 (49.04)	3.91 (3.83)	13.00 (12.52)	9.20 (9.06)	7.50 (7.15)	Brown	60	>220 Decomposition	59.0
$[Fe_2(L)_4(Cl)_2]\cdot 3H_2O$[c], $C_{64}H_{50}N_{12}O_7Cl_6$ Fe_2 (1423)	54.44 (53.97)	4.00 (3.51)	12.10 (11.80)	15.10 (14.96)	8.70 (7.78)	Brownish-black	66	>260 Decomposition	3.6
$[Fe(L)(8\text{-}OHqu(Cl)(H_2O)]\cdot 2H_2O$[b], $C_{25}H_{23}N_4O_6Cl_2$ Fe (602)	50.20 (49.83)	4.82 (3.82)	10.00 (9.30)	12.05 (11.79)	10.20 (9.30)	Brown	70	>260 Decomposition	80
$[Co(L)_2(OH_2)_2]\cdot 3H_2O$, $C_{32}H_{30}N_6O_8Cl$ Co (706.5)	53.03 (54.35)	4.14 (4.24)	11.60 (11.88)	4.90 (5.02)	8.22 (8.35)	Yellowish brown	70	>250 Decomposition	1.9
$[UO_2(L)_2(OH_2)]\cdot 2H_2O$, $C_{32}H_{28}N_6O_7Cl_2$ U (917)	42.12 (41.87)	3.35 (3.05)	9.52 (9.16)	8.1 (7.74)	26.5 (25.90	Orange	72	>230 Decomposition	3.7

[a] Measured at ambient temperature for 1×10^{-3} M in DMF (Ω^{-1} cm^2 mol^{-1}).

[b] Mixed ligand complexes.

[c] Obtained from the reaction of the ligand and Fe(III) in presence of LiOH.

Table 2
^1H NMR data of the ligand HL in DMF-d_6

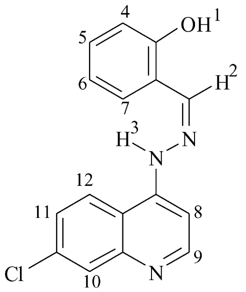

7-Chloro-4-(*o*-hydroxybenzylidinehydrazo)quinoline, HL

Chemical shift, δ_{TMS} (ppm)	Assignment[a]
14.5	[s, 1H] (1)
6.2	[s, 1H] (2)
11.7	[s, 1H] (3)
7.9–8.3	[m, 9H, Ar–H, and quinoline–H]

[a] s, singlet and m, multiplet.

efficiencies of the investigated metal complexes. The prepared compounds were tested against one strain of Gram positive bacteria (*Staphylococcus aureu*), Gram negative bacteria (*Escherichia coli*), and fungi (*Candida albicans*) to provide the minimum inhibitory concentration (MIC's) for each complex. Bacteriostatic and fungistatic efficiency is the lowest concentration of solution to inhibit the growth of a test organism.

3. Results and discussion

3.1. The organic ligand, HL

Elemental analyses (Table 1) of the ligand reflected that the ligand has molecular formula given. The ^1H NMR spectrum (Table 2) of the ligand in deuterated dimethylformamide showed two signals at $\delta = 14.5$ and 11.7 ppm for the proton of the phenolic OH and the NH groups, respectively. A signal is also observed at $\delta = 6.62$ ppm for the HC=N– group [20] (Table 2). Addition of D_2O to the previous solution results in diminishing the signals due to the protons of phenolic OH and HN–N groups.

The IR spectrum of the ligand (Table 3) shows a strong band at 3530 cm^{-1} assigned to νOH of the phenolic group. The stretching vibration of NH group appears as weak bands at 3300 cm^{-1}. The spectrum shows also vibrational bands at 1605, 1600, and 1140 and 1130 cm^{-1} assigned for ν_s and ν_{as} of the C=N and N–N groups, respectively. The deformation vibration, δ, of the phenolic OH group appears at 1278 cm^{-1}. The vibrational band observed at 2570 cm^{-1} could be assigned for the intramolecular hydrogen bonding.

The UV–vis spectrum (Table 4) recorded for the ethanolic solution of the ligand showed absorption bands at 48,076 and 44,642 cm^{-1} assigned for π–π^* transitions within the aromatic and quinoline rings. The band observed at 36,231 cm^{-1} would be due to the n–π^* transition of the C=N group. The absorption bands at 26,176 and 24,752 cm^{-1} are assigned for CT transitions. The band at 24,752 cm^{-1} encroaches on the visible region [21] and impacts the ligand and its colour.

Table 3
Characteristic IR bands (cm^{-1}) of HL and its corresponding metal complexes

Compound, M.F. (M.Wt.)	ν(C=N)	ν(N—H)	ν(N–N)	ν(M–N)	ν(M–O)	ν(OH), H_2O	Other bands
HL_a, $C_{16}H_{12}N_3OCl$ (297.5)	1605 s	3300 w	1140 s	–	–	3530 (νOH–phenolic)	1600 $\nu(C{=}N)_{as}$, 1130 $\nu(N–N)_{as}$, 1278 (δ OH–phenolic)
$[Cu(L)_2]\cdot H_2O$, $C_{32}H_{24}N_6O_3Cl_2$ Cu (674.5)	1595 s	3214 w, br	1136 s	420 w	540 m	3380 (lattice water)	
$[Cu(L)(8\text{-}OHqu)]\cdot H_2O$, $C_{25}H_{19}N_4O_3Cl$ Cu (522)	1597 m	3200 s	1137 w	425 w	520 m	3380 (lattice water)	
$[Ni(L)_2(OH_2)_2]\cdot 3H_2O$, $C_{32}H_{32}N_6O_7Cl_2$ Ni (742)	1597 s	3215 w	1125 w	410 w	515 m	3380 (lattice water), 3495 (coordinated water)	
$[Ni(L)(8\text{-}OHqu)]\cdot 3H_2O$, $C_{25}H_{23}N_4O_5Cl$ Ni (553.5)	1598 m	3210 w	1136 s	445 w	520 w	3375 (lattice water)	
$[Fe(L)_2(OH_2)_2]\cdot NO_3\cdot 2H_2O$, $C_{32}H_{30}N_7O_9Cl_2$ Fe (783)	1594 s	3214 w, br	1137 s	465 w	520 m	3385 (lattice water), 3490 (coordinated water)	1385 s, 835 s, 710 m (νNO_3)
$[Fe_2(L)_4(Cl)_2]\cdot 3H_2O$, $C_{64}H_{50}N_{12}O_7Cl_6$ Fe_2 (1423)	1597 s	3211 w	1134 s	460 w	540 w	3390 (lattice water)	
$[Fe(L)(8\text{-}OHqu(Cl)(H_2O)]\cdot 2H_2O$, $C_{25}H_{23}N_4O_6Cl_2$ Fe (602)	1597 s	3218 w	1138 w	460 w	515 w	3380 (lattice water), 3495 (coordinated water)	
$[Co(L)_2(OH_2)_2]\cdot 3H_2O$, $C_{32}H_{30}N_6O_8Cl$ Co (706.5)	1597 m	3222 w	1145 s	465 w	540 m	3390 (lattice water), 3490 (coordinated water)	
$[UO_2(L)_2(OH_2)]\cdot 2H_2O$, $C_{32}H_{28}N_6O_7Cl_2$ U (917)	1595 s	3214 w	1140 s	465 w	530 m	3390 (lattice water), 3495 (coordinated water)	906 s ($\nu U^{(VI)}O_2$)

s: strong, w: weak, m: medium, and br: broad.

The mass spectrum of the ligand (Fig. 1) showed its molecular ion at *m*/*e* 297 which coincides with formula weight. Metastable ion(s) is not observed. Scheme 1 represents the proposed fragmentation pattern of the ligand.

The pH-metric measurement for 3×10^{-3} M of 75% (v/v) ethanol–water solution of the ligand indicated that only one proton dissociates together with the value of pK_a (10.63) suggesting that the ligand behaves as a weak monoprotic acid. The value of pK_a reveals that the proton dissociated from the phenolic OH group rather than from the N-proton of the hydrazino moiety which may dissociated at higher pH region.

Elemental analyses and IR spectra of ligand and its metal complexes under investigation (Tables 1 and 3) showed that the HL coordinated with the metal ions as monoprotic bidentate ligand and its coordination mode could be represented as shown in Fig. 2.

3.2. Metal complexes

Table 1 shows the elemental analyses and molecular formula of the complexes obtained from the reaction of the Schiff base hydrazone ligand, HL, with the transition metal ions, Cu(II), Ni(II), Co(II), UO_2(II), and Fe(III), in the molar ratio 1:1 (M:L). The reactions were carried out in presence and in absence of LiOH as deprotonating agent. In all cases, except for Fe(III) ion, only one product obtained indicating that the presence of LiOH does not affect the formation of the complexes. The exception is Fe(III) ion, where two complexes were

Table 4
Magnetic moment, molar conductance, and electronic spectral data (cm^{-1}) for HL and its metal complexes

Compound, M.F. (M.Wt.)	μ_{eff} (B.M.)	$\pi \to \pi^*$, $n \to \pi^*$, and charge transfer transitions[a] (cm^{-1})	$d \to d$ transitions[a] (cm^{-1})
HL, $C_{16}H_{12}N_3OCl$ (297.5)	dia[b]	48067, 44642, 36231, 26176, 24752	–
$[Cu(L)_2]\cdot H_2O$, $C_{32}H_{24}N_6O_3Cl_2$ Cu (674.5)	1.75	36765, 28612, 22396	15520
$[Cu(L)(8\text{-}OHqu)]\cdot H_2O$, $C_{25}H_{19}N_4O_3Cl$ Cu (522)	1.80	36630, 28129, 22446	15850
$[Ni(L)_2(OH_2)_2]\cdot 3H_2O$, $C_{32}H_{32}N_6O_7Cl_2$ Ni (742)	2.85	37037, 28653, 22371	16220
$[Ni(L)(8\text{-}OHqu)]\cdot 3H_2O$, $C_{25}H_{23}N_4O_5Cl$ Ni (553.5)	3.02	37037, 28653, 22371	14599, 15058
$[Fe(L)_2(OH_2)_2]\cdot NO_3\cdot 2H_2O$, $C_{32}H_{30}N_7O_9Cl_2$ Fe (783)	5.40	35906, 28248, 25707, 21459	14050
$[Fe(L)(8\text{-}OHqu(Cl)(H_2O)]\cdot 2H_2O$[a], $C_{25}H_{23}N_4O_6Cl_2$ Fe (602)	5.65	35971, 27701, 25252, 20230	14050
$[Fe_2(L)_4(Cl)_2]\cdot 3H_2O$[a], $C_{64}H_{50}N_{12}O_7Cl_6$ Fe_2 (1423)	7.25	35971, 27701, 25252, 20230	14331, 13850
$[Co(L)_2(OH_2)_2]\cdot 3H_2O$, $C_{32}H_{30}N_6O_8Cl$ Co (706.5)	5.08	37037, 28449, 22421	18.480, 15390
$[UO_2(L)_2(OH_2)]\cdot 2H_2O$, $C_{32}H_{28}N_6O_7Cl_2$ U (917)	dia[b]	37147, 27956, 22371	–

[a] As Nujol mull.

[b] dia, diamagnetic.

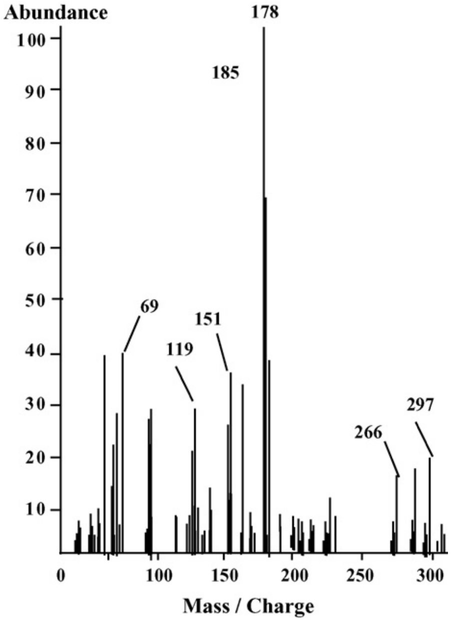

Fig. 1. Mass spectrum of HL recorded at 300 °C and 70 eV.

obtained in the presence and absence of LiOH. This could be attributed to the aggregate tendency of Fe(III) ion. The table represents, also, the obtained mixed ligand complexes from the reaction mixture of Cu(II), Ni(II), and Fe(III) with HL and 8-OHqu in the presence of LiOH in the molar ratio 1:1:1:1 (M:HL:8-OHqu:LiOH).

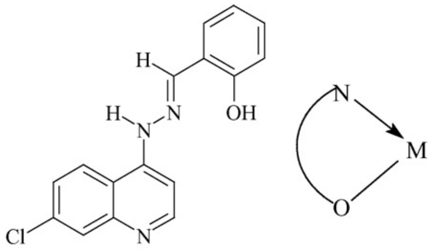

Fig. 2. Mode of coordination sites of the ligand HL.

3.3. The IR spectra of the metal complexes

The IR spectra (Table 3) of the metal complexes showed that the band due to phenolic OH group that appeared in the spectrum of the ligand at 3530 cm^{-1} has disappeared in the spectra of the complexes, which may be due to the displacement of its proton by the metal ion in accordance with the pH-metric and dissociation constant of the ligand. Moreover, the spectra showed that the vibrations of –C=N group were shifted to a lower frequency due to the coordination of the nitrogen atom of the azomethine group. As a result, the Schiff base hydrazone ligand, HL, coordinates in all complexes as monoprotic bidentate ON ligand via the oxygen atom of the phenolic OH and the nitrogen atom of the azomethine groups [22]. Similar results were obtained from the IR spectra of the mixed 8-hydroxyquinoline complexes (Table 3) in which the frequency of the C_8–OH group does not appear due to the replacement of the proton of the OH by the metal ion, and the lowering in the frequency of the azomethine group due to

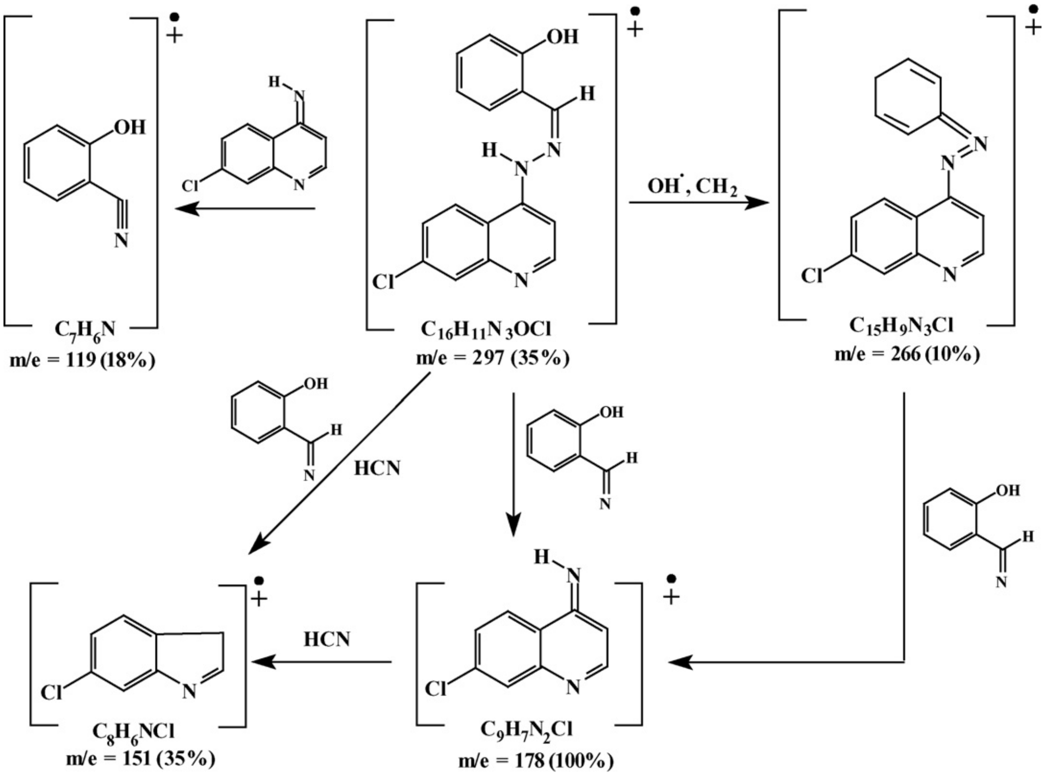

Scheme 1. Proposed mass fragmentation pattern of HL.

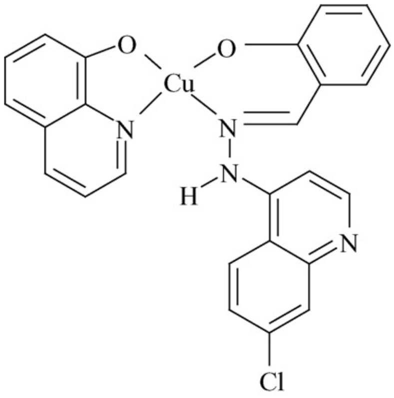

Fig. 3. Proposed structures of square-planar geometry of [Cu(L)(8-OHqu)] complex.

the coordination of the nitrogen atom of the quinoline moiety with the metal ions [22]. In all spectra, new bands appeared, for all types of the complexes, at 515–540 and 410–465 cm^{-1}, that would be assigned to νM–O and νM–N, respectively.

3.4. Magnetic moments and electronic spectra of the metal complexes

The electronic spectra and magnetic moment of the metal complexes are listed in Table 4. Generally, in all spectra of metal complexes, the absorption bands due to π–π^* and n–π^* transitions that are observed in the spectrum of the free ligand higher than 22,300 cm^{-1} have shifted to lower frequencies due to the coordination of the ligand with metal ions.

The spectra of $[Cu(L)_2]\cdot H_2O$ and $[Cu(L)(8\text{-OHqu})]\cdot H_2O$ complexes showed absorption bands at 15,520–15,850 cm^{-1} which could be attributed to the $^2A_{1g} \rightarrow {}^2B_{1g}$ transitions characterized by Cu(II) ion in a square-planar geometry [23–25]. The square-planar geometry [23–25] of Cu(II) ion in both complexes (Fig. 3) is confirmed by the measured magnetic moments values, 1.75 and 1.80 B.M., respectively. The square-planar geometry is achieved by the coordination of two molecules of HL or through one molecule of HL $[Cu(L)_2]\cdot H_2O$ and one molecule of 8-OHqu in the mixed ligand complex $[Cu(L)(8\text{-OHqu})]\cdot H_2O$.

The electronic spectrum of the $[Ni(L)_2(OH_2)_2]\cdot 3H_2O$ complex showed broad absorption band at 16,220 cm^{-1} which may be assigned to $^3A_{1g}(F) \rightarrow {}^3T_{2g}(F)$, while the absorption due to $^3A_{2g}(F) \rightarrow {}^3T_{1g}(P)$ (Table 4) is overlapped with the ligand absorption bands. This indicates that the Ni(II) ion coordinated to N_2O_2 sites in an octahedral geometry (Fig. 4). The Ni(II) ion completes its six-coordination sphere by two water molecules. The third transition due to $^3A_{2g}(F) \rightarrow {}^3T_{1g}(P)$ would be out of scale of the used spectrophotometer [26]. The magnetic moment of the complex is 2.85 B.M. which agrees with the presence of Ni(II) ion in octahedral geometry [27,28].

On the other hand, the spectrum of $[Ni(L)(8\text{-OHqu})]\cdot 3H_2O$ complex showed absorption bands at 14,599 and 15,058 cm^{-1} arising from the $^3T_1(F) \rightarrow {}^3A_2(F)$ transitions characterized by Ni(II) ion in a tetrahedral environment which agrees with the electron spectrum of $[NiCl_4]^{2-}$. The tetrahedral geometry is confirmed by the measured magnetic moment ($\mu_{eff} = 3.02$ B.M.) which is in harmony with the reported [24] value, $\mu_{eff} = 3.07$ B.M., for the tetrahedral complex $NiCl_2(PPh_3)_2$.

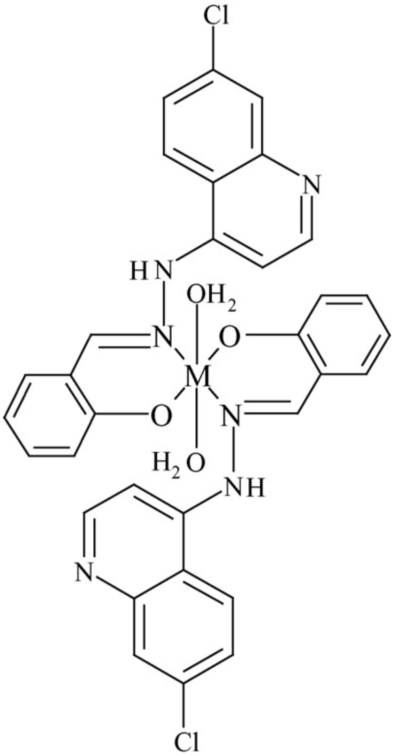

Fig. 4. Proposed octahedral structures of $[M(L)_2(OH_2)_2]$, where M = Cu, Ni, Co, and Fe.

The electronic spectra of $[Fe(L)_2(OH_2)_2]\cdot NO_3\cdot 2H_2O$ and $[Fe(L)(8\text{-OHqu})(Cl)(H_2O)]\cdot 2H_2O$ complexes showed bands at 13,230–14,050 and 19,830–20,680 cm^{-1} assigned for $^6A_{1g} \rightarrow {}^4T_{2g}(G)$ and $^6A_1(G) \rightarrow {}^4T_1(G)$ transitions. These results together with measured magnetic moments for both complexes 5.40 and 5.65 B.M., respectively, are compatible with those reported for octahedral geometry around Fe(III) ions [29].

On the other hand, the electronic spectrum of $[Fe_2(L)_4(Cl)_2]\cdot 3H_2O$ showed broad bands at 14,331 and 13,850 cm^{-1}. The former band may be due to the spin forbidden transition $^6A_{1g} \rightarrow {}^4T_{2g}(G)$, which may gain intensity as a result of the vibronic mechanism in the octahedral field around ferric ion (Fig. 5). The second band may be attributed to $^6A_1 \rightarrow {}^4T_1(G)$ transitions [29]. In addition, a third absorption band with a high intensity observed at 25,252 cm^{-1} is assigned for charge transfer transition. The magnetic moment of complex is 7.25 B.M. This value is quite low compared to the calculated magnetic moment value for binuclear ion complex.

Octahedral, tetrahedral and square-planar cobalt(II) complexes show magnetic moment [30] between 4.7 and 5.2, 4.2 and 4.8, and 2.2 and 2.9 B.M., respectively. The μ_{eff} value measured for the present $[Co(L)_2(OH_2)_2]\cdot 3H_2O$ complex (Table 4) is 5.08 B.M. which is fairly close to those reported [30] for the unpaired electrons for Co(II) ion in an octahedral environment (Fig. 4). The electronic spectrum of the complex showed two d–d transitions in the range 15,250–15,390 cm^{-1} and

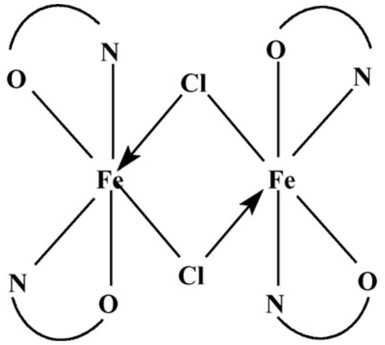

Fig. 5. Proposed structures of bridged octahedral geometry of $[Fe_2(L)_4(Cl)_2]$ complex.

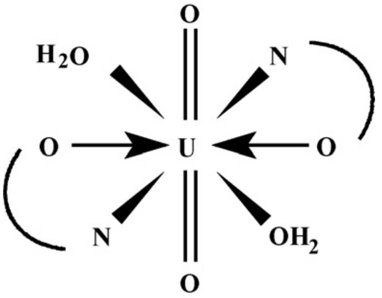

Fig. 6. Tentative structure of $[UO_2(L)_2(OH_2)]$ complex.

18,410–18,480 cm^{-1} due to the transitions $^4T_{1g}(F) \rightarrow {}^4A_{2g}(F)$ and $^4T_{1g}(F) \rightarrow {}^4A_{2g}(P)$, respectively, indicating an octahedral configuration around Co(II). The $^4T_{2g}(F) \rightarrow {}^4T_{1g}(F)$ transition (9510 cm^{-1}) would be observed in near IR region [31]. This region is out of scale of our spectrophotometer.

The electronic spectra of the diamagnetic uranyl complex, $[UO_2(L)_2(OH_2)]\cdot 2H_2O$ (Fig. 6), show two bands, in addition to the ligand bands. The first band is observed at 22,500 cm^{-1} corresponding to charge transfer from equatorial donor atoms of the ligand to the uranyl ion. The second band is observed at 19,040 cm^{-1} due to electronic transitions from apical oxygen atom to the f-orbitals of the uranyl atom characteristic of the uranyl moiety [32].

3.5. Molar conductance of the metal complexes

The conductance measurements, recorded for 10^{-3} M solutions of the metal complexes in DMF, are listed in Table 1. All complexes, except two, are non-conducting and the measured molar conductance ranged from 2.0 to 3.6 Ω^{-1} cm^2 mol^{-1} indicating their neutrality and the divalent metal cations replaced the phenolic proton. The exceptions are $[Fe(L)_2(OH_2)_2]\cdot NO_3\cdot 2H_2O$ and $[Fe_2(L)_4(Cl)_2]\cdot 3H_2O$ complexes which showed molar conductance of 80.0 and 59.0 Ω^{-1} cm^2 mol^{-1}, respectively, indicating their electrolytic nature as 1:1 electrolyte for the former complex while the electrolytic nature of the second complex may be due to the replacement of the coordinated chloride ions by solvent molecules, a phenomenon usually encountered in complexes containing chloride ions [33].

3.6. ^{1}H NMR spectrum of the uranyl complex

The uranyl complex was selected as it is diamagnetic. Its ^{1}H NMR spectra in DMF and after deuteration are discussed. The spectrum of the complex differs from that of the free ligand in the following aspects:

Table 5
Thermal analyses data for some metal complexes of HL

Compound, M.F. (M.Wt.)	Dissociation stages	Temperature range in TG (°C)	Weight loss found (calculated) (%)	Decomposition assignment
$[Cu(L)_2]\cdot H_2O$, $C_{32}H_{24}N_6O_3Cl_2$ Cu (674.5)	Stage I	41–98	2.46 (2.67)	1 mol lattice H_2O
	Stage II	233.5–383.9	41.95 (41.79)	C_7H_5N and $C_9H_7N_2Cl$
	Stage III	385.8–645.0	15.35 (15.36)	C_6H_5N and C_9H_7NCl
	Stage IV	646.0–795.4	14.86 (11.7)	Formation of CuO
$[Ni(L)_2(OH_2)_2]\cdot 3H_2O$[a], $C_{32}H_{32}N_6O_7Cl_2$ Ni (742)	Stage I	37–89	7.51 (7.27)	3 mol lattice H_2O
	Stage II	129.3–243.5	28.70 (28.90)	2 mol coord. H_2O, $C_9H_7N_2Cl$
	Stage III	244.6–290.9	27.97 (27.77)	2 C_6H_5N
	Stage IV	292.9–538.9	23.98 (24.06)	$C_9H_7N_2Cl$
	Stage V	539.9–796.8	12.98 (10.10)	Formation of NiO
$[Fe(L)_2(OH_2)_2]\cdot NO_3\cdot 2H_2O$, $C_{32}H_{30}N_7O_9Cl_2$ Fe (783)	Stage I	34.4–98	4.43 (4.60)	2 mol lattice H_2O
	Stage II	195.4–250.4	25.56 (2.59)	2 mol coord. H_2O, C_6H_5N, NO_3
	Stage III	251.5–489.9	13.13 (13.71)	C_6H_5N
	Stage IV	491.9–643.9	22.90 (22.76)	2 mol $C_9H_7N_2Cl$
	Stage V	644.9–795.7	23.97 (20.86)	Formation of Fe_2O_3

[a] Complex $[Co(L)_2(OH_2)_2]\cdot 3H_2O$ exhibited the same decomposition pattern.

Table 6
Results of antimicrobial activity of some tested complexes

Compound	Concentration (%)	Microorganism		
		Staphylococcus aureus (ATCC[a] 6538, MIC[b] 25%)	*Escherichia coli* (ATCC 8739, MIC 25%)	*Candida albicans* (ATCC 10231, MIC 25%)
7-Chloro-4-(*o*-hydroxybenzilidenehydrazo)quinoline, HL	1[c]			
	25	Positive	Positive	Positive
	50	Positive	Positive	Positive
	100	Negative	Positive	Positive
$[Ni(L)_2(OH_2)_2]\cdot 3H_2O$	1	Positive	Positive	Positive
	25	Negative	Negative	Negative
	50	Negative	Negative	Negative
	100	Negative	Negative	Negative
$[Fe(L)_2(OH_2)_2]\cdot NO_3\cdot 2H_2O$	1	Positive	Positive	Positive
	25	Negative	Negative	Negative
	50	Negative	Negative	Negative
	100	Negative	Negative	Negative
7-Chloro-4-hydrazinoquinoline	1[c]			
	25	Negative	Positive	Negative
	50	Negative	Negative	Negative
	100	Negative	Negative	Negative
$[Co(L)_2(OH_2)_2]\cdot 3H_2O$	1	Positive	Positive	Positive
	25	Negative	Negative	Negative
	50	Negative	Negative	Negative
	100	Negative	Positive	Negative
$[UO_2(L)_2(OH_2)]\cdot 2H_2O$	25	Negative	Negative	Negative
	50	Negative	Negative	Negative
	100	Negative	Positive	Negative

Key to symbols—Active and inhibit the growth of the stain: negative; inactive: positive.

[a] Number of stain in the American collection.

[b] MIC is the lowest concentration of the product material solution to inhibit the growth of the microorganism.

[c] Not tested in this concentration.

1. The disappearance of the signal due to the phenolic OH group is attributed to its involvement in coordinating the uranyl cation, while the signal due to the NH group was broad and appeared at $\delta = 12.4$ ppm compared to that of the ligand which appeared at $\delta = 11.7$ ppm, i.e. shifted to low-field.
2. The signals due to the aramaic ring showed fine structure and appear as four separate signals at $\delta = 6.53$, 6.67, 7.14, and 7.6 ppm.
3. A new signal for coordinated water appeared at $\delta = 3.4$ ppm.

3.7. Thermal analyses

The TG–DTA results of the solid complexes, $[Cu(L)_2]\cdot H_2O$, $[Ni(L)_2(OH_2)_2]\cdot 3H_2O$, and $[Fe(L)_2(OH_2)_2]\cdot NO_3\cdot 2H_2O$, are listed in Table 5. The results show good agreement with the formulae suggested from the analytical data (Table 1). A general decomposition pattern was concluded in which the complexes decomposed in four stages. Besides the four stages, complexes, which have coordinated water, exhibited additional stage to be decomposed in five stages (Table 5). Complexes with lattice water become anhydrous at 41–98 °C. The second stage is the loss of the coordinated water molecules at 130–250 °C and in some cases loss of part of the organic ligand accompanying the removal of coordinated water in this stage. The third to fifth stages represented the loss of the rest of the organic moiety and the formation of metal oxides.

3.8. Antimicrobial activity and minimum inhibitory concentration

The test was performed according to the method reported previously [34]. 0.02 g of each complex was dissolved in 100 ml dimethylsulfoxide, DMSO, to produce 0.02% solutions. To a series of culture tubes, in which each tube contains sterile 5 ml double strength solution of Soyabean Casein Digest Medium (Tryptic Soy Broth), 5 ml of the 0.02% DMS solution was added to each tube and mixed. To determine the bacteriostatic efficiency of the *S. aureu* and *E. coli* organisms, 1 ml of a 1:10 diluted solution of Tryptic Soy Broth (TSB) was added to each culture tube. A 1:10 diluted solution of Tryptic Soy Broth was prepared by pipetting 1 ml of bacterial cultures incubated at 37 °C for 24 h into 9 ml of sterile Tryptic Soy Broth. For the test of the fungistatical efficiency, 0.1 ml of undiluted sample incubated for 72 h at 37 °C TSB cultivation of *C. albicans* was used. All inoculated culture tubes were incubated at 30–35 °C for 18–24 h. After that, the “MIC” level was assessed visually.

MIC was recorded as the first clear tubes after turbidity, starting with the blank broth. In other words, the highest dilution of the antiseptic/disinfectant preventing growth is taken as the "MIC" of the test organism [34].

The tests were carried out for concentrations of 1, 25, 50, and 100% DMSO solutions of the compounds. The inhibition zones caused by the various compounds on the microorganisms were examined. The results of the preliminary screening test are listed in Table 6. From the data obtained in Table 4, it is clear that 7-chloro-4-hydrazinoquinoline was found to be highly active against all organisms and in all concentrations while 7-chloro-4-(*o*-hydroxybenzilidenehydrazo)quinolene exhibited its activity at its 100% concentration for only *S. aureu* and does not affect the other tested stained organisms in all of its concentration. Remarkable result is that the complexes, $[Ni(L)_2(OH_2)_2]\cdot 3H_2O$, $[Co(L)_2(OH_2)_2]\cdot 3H_2O$, and $[Fe(L)_2(OH_2)_2]\cdot NO_3\cdot 2H_2O$, were found to have high activity against all stains in all of their concentrations except their 1% concentration. On the other hand, $[UO_2(L)_2(OH_2)]\cdot 2H_2O$ was found to have higher activity against stains *Staphylococcus aureus* and *C. albicans* in its 25, 50, and 100% concentrations, while for *E. coli*, its activity was exhibited for 25 and 50% concentrations. The tested compounds showed an inhibitory activity of 25%.

4. Conclusion

The results of this investigation support the suggested structures of the metal complexes. In case of Cu(II), Ni(II), Co(II), and UO_2(II) cations, only mononuclear complexes were obtained in presence and absence of LiOH indicating that the presence of LiOH does not affect the formation of such complexes. On the other hand, two Fe(III) complexes, mono- and binuclear, were obtained in the absence and presence of LiOH, respectively, during their preparation as mentioned in Section 2. All metal cations, Cu(II), Ni(II), Co(II), and Fe(III), were octahedral, while Cu(II) and Ni(II) cations in mixed ligand complexes proved an extra square-planar and tetrahedral geometries, respectively. Binuclear complexes of Fe(III) have octahedral structure in which the two Fe(III) cations are bridged by two chlorine atoms.

References

[1] Z.H. Chohan, S.K.A. Sheazi, Synth. React. Inorg. Met. Org. Chem. 29 (1999) 105.
[2] C. Jayabalakrishnan, K. Natarajan, Synth. React. Inorg. Met. Org. Chem. 31 (2001) 983.
[3] T. Jeeworth, H.L.K. Wah, M.G. Bhowon, D. Ghoorhoo, K. Babooram, Synth. React. Inorg. Met. Org. Chem. 30 (2000) 1023.
[4] N. Dharmaraj, P. Viswanalhamurthi, K. Natarajan, Transition Met. Chem. 26 (2001) 105.
[5] C.H. Colins, P.M. Lyne, Microhiul Methods, University Park Press, Baltimore, 1970, p. 422.
[6] L. Savanini, L. Chiasserini, A. Gaeta, C. Pellerano, Biorganic and Medical Chemistry 10 (2002) 2193.
[7] E. Ochiai, Bioinorganic Chemistry, Allyn and Bacon, Boston, 1977.
[8] J.A. Anten, D. Nicholis, J.M. Markpoulos, O. Markopoulou, Polyhedron 6 (1987) 1074.
[9] I.A. Tossadis, C.A. Bolos, P.N. Aslanidis, G.A. Katsoulos, Inorg. Chim. Acta 133 (1987) 275.
[10] A. Maiti, S. Ghosh, Indian J. Chem. 28A (1989) 980.
[11] R.C. Aggarwal, N.K. Singh, R.P. Singh, Inorg. Chim. Acta 29 (1981) 2794.
[12] J.C. Craliz, J.C. Rub, D. Willis, J. Edger, Nature 34 (1955) 176.
[13] J.R. Dilworth, Coord. Chem. Rev. 21 (1976) 29.
[14] J.R. Merchant, D.S. Clothia, J. Med. Chem. 13 (1970) 335.
[15] N.S. Biradar, B.R. Havinale, Inorg. Chim. Acta 17 (1976) 157.
[16] H.N. Fox, Science 116 (1952) 129.
[17] S. Kakimoto, K. Yashamoto, Pharm. Bull. 4 (1956) 4.
[18] R.K. Agarwal, R.K. Sarin, Polyhedron 12 (1993) 241.
[19] G. Durgaprasad, C.C. Patel, Indian J. Chem. 11A (1973) 1300.
[20] R.M. Silverstein, G.C. Bassler, C. Morill, Spectrometric Identification of Organic Compound, fourth ed., John Wiley, New York, 1981.
[21] K. Ueno, A.E. Martell, J. Chem. Phys. 61 (1957) 257.
[22] C. Dreti, G. Tosi, Aust. J. Chem. 29 (1996) 543.
[23] B.N. Figgs, J. Lewis, Prog. Inorg. Chem. 37 (1964) 67.
[24] B.N. Figgs, Introduction to Ligand Field, Wiley, New York, 1966, pp. 203; A.B.P. Lever, Inorganic Electronic Spectroscopy, second ed., Elsevier, Amsterdam, 1984.
[25] A. Symal, K.S. Kale, Indian J. Chem., Sect. A 16 (1978) 46.
[26] J.C. Bailar, H.H. Emeleus, R. Nyholm, A.F. Trotman-Dickenson (Eds.), Comprehensive Inorganic Chemistry, vol. 3, Pergamon Press, Oxford, 1975, pp. 1088.
[27] M.M. Patel, R. Manvalan, J. Macromol. Sci. Chem. 19 (1973) 951.
[28] A.S. Aswar, R.G. Mahale, P.R. Kakde, S.Q. Bhadange, J. Indian Chem. Soc. 75 (1998) 395.
[29] K. Dey, J. Indian Chem. Soc. 48 (1971) 641.
[30] G. Dyer, D.W. Meek, J. Am. Chem. Soc. 81 (1967) 3983.
[31] F.A. Cotton, G. Wilkinson, Advanced Inorganic Chemistry, third ed., Inter Science Publishers, New York, 1972, pp. 538.
[32] A. Lal, K. Sigh, N. Siva, S. Adhikari, S. Yadav, Synth. React. Inorg. Met. Org. Chem. 26 (1996) 321.
[33] M.E. Balewin, J. Chem. Soc. 3123 (1961);
S.J. Gruber, C.M. Harris, E. Sinn, J. Inorg. Nucl. Chem. 30 (1968) 1805.
[34] H. William, V. Stephen, Theory and Application of Microbiological Assay, Academic Press, San Diego, 1989, p. 320.